

# Viscoelasticity and Processability of a BAMO/AMMO Thermoplastic Elastomer

By R. E. Kucukpinar and Dilhan M. Kalyon

Chemical Engineering Department and Highly Filled Materials Institute  
Hoboken, New Jersey

## INTRODUCTION

Thermoplastic elastomer based formulations are used widely in various applications, traditionally served by vulcanized rubbers and other thermosetting polymers. The ability to use conventional polymer processing equipment including injection and transfer molders and extruders and recyclability provide additional incentives. However, such processing operations also require detailed information on the rheological behavior of the thermoplastic elastomer and processability analysis. In this study, we provide extensive data on various viscoelastic material functions of a melt of a BAMO/AMMO based thermoplastic elastomer used in conjunction with a non-linear constitutive equation to enable predictions of rheological behavior and processability under conditions relevant to various molding and extrusion operations.

## MATERIALS

A recently introduced thermoplastic elastomer based on a BAMO-AMMO copolymer was produced from Thiokol Corporation. BAMO-AMMO is an alternating block copolymer obtained from the polymerization of BAMO and AMMO monomers. BAMO (3,3-bis(azidomethyl)oxetane) is a crystalline homopolymer forming the hard block and AMMO (3-azidomethyl-oxetane) is an amorphous homopolymer forming the soft block of the energetic thermoplastic elastomer. In this study BAMO-AMMO with a 25% BAMO is characterized. The melting temperature of BAMO-AMMO is 74.8 °C. This thermoplastic elastomer has a number average molecular weight of 10600 and a weight-average molecular weight of 45400, as reported by the manufacturer, Thiokol Corporation.

## RHEOLOGICAL CHARACTERIZATION

The BAMO-AMMO thermoplastic elastomer was first characterized in terms of its linear viscoelastic properties, storage ( $G'$ ) and loss ( $G''$ ) moduli employing a Rheometric Scientific System IV in conjunction with 25-mm diameter parallel-plate fixtures. The experiments were carried out in the 85-100 °C range. The material is stable under the employed temperatures. The small amplitude oscillatory shear experiments covered the 0.01 to 100 rps frequency range. The magnitude of the complex viscosity,  $|\eta^*|$  was determined from:

$$|\eta^*(\omega)| = ((G'/\omega)^2 + (G''/\omega)^2)^{0.5} \quad (1)$$

The Rheometrics System IV was again used for steady shear, stress growth, and stress relaxation experiments, in conjunction with 25-mm cone and plate fixtures. Furthermore, a series of stress relaxation after sudden shearing displacement experiments were carried out in the 25-1200% strain range to determine the relaxation moduli,  $G(t, \gamma_0)$ :

$$G(t, \gamma_0) = \tau_{xy}(t) / \gamma_0 \quad (2a)$$

where  $\tau_{xy}(t)$  is the shear stress and  $\gamma_0$  is the imposed shear strain. In these experiments parallel-plate fixtures were employed. The parallel plate data were corrected by employing (1,2):

$$G(t, \gamma_R) = G_a(t, \gamma_R) \left[ 1 + \frac{1}{4} \frac{\partial \ln G_a(t, \gamma_R)}{\partial \ln \gamma_R} \right] \quad (2b)$$

where  $\gamma_R$  is the strain at the edge of the disk,  $R$ , and  $t$  is time. The apparent modulus  $G_a(t, \gamma_R)$  is given as:

$$G_a(t, \gamma_R) = \frac{2Y(t, \gamma_R)}{\pi R^3 \gamma_R} \quad (2c)$$

and strain at radius  $R$ :

$$\gamma_R = \frac{\theta R}{H} \quad (2d)$$

where  $\theta$  is the angular displacement,  $R$  and  $H$  are the radius of the disk and the gap separation between the two disks, respectively, and  $Y$  is the torque exerted by the thermoplastic elastomer on the disk. The rise times involved in the imposition of the strain,  $\gamma_R$ , were not negligible in our experiments and varied between 0.1 to 0.8 s. The relaxation modulus values were corrected for the rise time on the basis of the procedure suggested by Laun (3).

### CONSTITUTIVE EQUATION

To gain insight into the processing behavior of these engineering thermoplastics the experimental data were employed to determine the material-dependent parameters of the following integral type, network-based equation fitting the general form (4):

$$\tau = \int_0^{\infty} \left[ M_1(s, I_1, I_2) \mathbf{C}_t^{-1} + M_2(s, I_1, I_2) \mathbf{C}_t \right] ds \quad (3)$$

where  $\mathbf{C}_{t-1}$  and  $\mathbf{C}_t$  are the Finger and Cauchy tensors, respectively, and  $M_1$  and  $M_2$  are the memory functions which are given as functions of the first,  $I_1$ , and second,  $I_2$  invariants of the Finger tensor and the elapsed time  $s$ . Here we have followed Wagner's postulate (5) by setting  $M_2$  to zero and assuming that the memory function,  $M_1$  can be expressed as a product of two functions:

$$M_1(s, I_1, I_2) = M_0(s)h(I_1, I_2) \quad (4)$$

where  $h(I_1, I_2) \leq 1$  is the temperature-independent damping function which tends to unity for small deformations and  $M_0(s)$  is the Lodge's rubberlike-liquid memory function (6):

$$M_0(s) = \sum_i (G_{0i} / \lambda_i) \exp(-(t-t') / \lambda_i) \quad (5)$$

where  $G_{0i}$  and  $\lambda_i$  are the relaxation strength and time, respectively and  $(t-t')$  is the elapsed time,  $s$ . We have employed a double exponential dependence of the damping function to strain (3,5) namely,

$$h(\gamma) = f \exp(-n_1 \gamma) + (1-f) \exp(-n_2 \gamma) \quad (6)$$

where  $f$ ,  $n_1$ , and  $n_2$  are material parameters. Various material functions predicted on the basis of this constitutive equation are reproduced here for convenience in Table 1.

### RESULTS AND DISCUSSION

The storage and loss moduli of the BAMO-AMMO (25% BAMO) are shown in Figure 1. The data were collected at 85, 90, 95,

100 °C. Assuming that the material is a thermorheologically simple fluid, the variations in temperature basically corresponds to a shift in time scale. Accordingly, all relaxation times change with temperature proportional to the shift factor,  $a_T$  (7).

$$\lambda_i(T) = a_T \lambda_i(T_0) \quad (7)$$

The relaxation strengths remain constant and the shift factor  $a_T$  is determined from the temperature dependence of magnitude of complex viscosity values determined at low frequency:

$$a_T(T) = \exp((E_a/R)(1/T - 1/T_0)) \quad (8)$$

where  $E_a$  is the activation energy and  $R$  is the gas constant. The activation energy for BAMO-AMMO (25% BAMO) was determined as 13.9 kcal/g-mol on the basis of equation (8). A reference temperature,  $T_0$  of 90 °C was selected. The discrete relaxation spectra for the resin were determined from the dynamic data employing a pattern search method that minimizes the objective function,  $F$  defined as:

$$F = \sum_{i=1}^N \left[ \left( \frac{G'_{i,exp} - G'_{i,fit}}{G'_{i,exp}} \right)^2 + \left( \frac{G''_{i,exp} - G''_{i,fit}}{G''_{i,exp}} \right)^2 \right] \quad (9)$$

where  $N$  is the number of data points,  $(G'_{i,exp}, G''_{i,exp})$  are available from the dynamic experiments and  $G'_{i,fit}, G''_{i,fit}$  denote the best fit values on the basis of Eqs. (11) and (12). The best fit of storage and loss moduli are shown in Figure 1 for the discrete spectra given in Table 2. The relaxation strengths  $G_{oi}$  represent the contribution to rigidity associated with relaxation times of the thermoplastic elastomer which lie in the interval  $\ln \lambda$  and  $\ln \lambda + d \ln \lambda$ .

The results of the step strain experiments are shown in Figures 2 and 3. In these experiments the broadest 95% confidence intervals determined according to Student's t-distribution were observed for the modulus values determined at small strains. This observed scatter should be related to the relatively small torques measured in this range. In the linear viscoelastic region, the shear relaxation modulus values can be related to the relaxation spectrum through:

$$G(t) = \sum_i G_{oi} \exp(-t / \lambda_i) \quad (10)$$

The relaxation moduli determined on the basis of Eq.(10) are indicated by the solid curve in Figure 2. The relaxation data pertaining to the linear viscoelastic range are further shown in Figure 3. The relaxation modulus values, which were determined according to Eq. (10) in the linear viscoelastic range, agree well with those determined employing step strain experiments.

The relaxation moduli values of BAMO-AMMO were determined up to a strain of 12, where the behavior is highly nonlinear. The relaxation moduli were separated into a time dependent modulus,  $G(t)$  determined in the linear viscoelastic range, and the strain dependent damping function,  $h(\gamma)$ , on the basis of Eq. (4). The damping function describes the destructive effect of the deformation in the entanglement density of the TPE melt. The damping function is given by the vertical shift required to superimpose the curves of relaxation modulus at various strains on the reference curve representing the linear viscoelastic region. For this TPE the curves of nonlinear relaxation modulus as a function of time for different strain levels were generally parallel for all times, as required by the time and strain separability. The factorization of the nonlinear relaxation modulus requires that the slopes of  $dG(t,\gamma)/dt$  be constant over the strain range. This is further elucidated in Figure 4 where the best fit of the damping function values collected at 0.25, 0.5, 0.75 s are compared. Mean values of the damping function values were also determined based on the best vertical shift of the nonlinear relaxation modulus curves over the entire experimental time range. The time dependence of the damping function is not strong. The three parameters of Eq. (6), which describe the strain dependence of the mean damping function values in shear flows, are reported in Table 3.

Figure 5 shows the typical comparison of the experimental shear stress growth behavior versus the predictions of the Wagner model. The comparisons of experimental and predicted stress relaxation upon the cessation of steady shear are reported in Figure 6. Overall, the agreement between the experimental and predicted time-dependent material functions is excellent. The predicted shear viscosity values are compared to the experimental values determined with cone and plate in Figure 7. The experimental magnitude of the complex viscosity values are also reported. According to the empirical Cox-Merz relationship (8), the

magnitude of the complex viscosity approximates the shear viscosity at corresponding values of shear rate and frequency at relatively small deformation rates. The ability to predict the shear viscosity material function over a broad range of shear rates and temperatures, applicable to various molding and extrusion flows, provides the basis necessary to predict the rheological behavior and processability of the TPE under relevant processing conditions and geometries.

## CONCLUSIONS

The rheological behavior of BAMO-AMMO (25% BAMO) was studied. The relaxation spectra and the damping function data were fitted in terms of a Wagner type BKZ model. The predictions of this model were compared with various viscometric material functions determined experimentally in this study. The reported experimental data and the model parameters should be helpful in defining the processing window of this elastomer and demonstrate techniques which are applicable to other types of thermoplastic elastomers.

## ACKNOWLEDGMENTS

This research was funded by the Office of Naval Research under contract N00014-95-1-0770 and under the direction of Dr. Richard S. Miller. We are grateful for this support. We are also grateful to NSWC and Mr. F. Gallant for making the materials of this study available and to Thiokol Corporation for their valuable input.

## References

1. R. Penn and E. Kearsley, *Trans. Soc. Rheol.*, 20, 2, 227 (1976).
2. P. Soskey and H. Winter, *J. Rheol.*, 28, 5, 625 (1984).
3. H. Laun, *Rheol. Acta*, 17, 1 (1978).
4. B. Bernstein, E. Kearsley, and L. Zapas, *Trans. Soc. Rheol.*, 7, 391 (1963).
5. M. H. Wagner, *Rheol. Acta*, 15, 136 (1976).
6. A. Lodge, *Trans. Faraday Soc.*, 52, 120 (1956).
7. J. Ferry, *Viscoelastic Properties of Polymers*, John Wiley, Third Edition, New York, 1980.
8. W. Cox and E. Merz, *J. Polym. Sci.*, 28, 619 (1958).

**Key Words:** Rheology, Thermoplastic elastomers, BAMO/AMMO

TABLE 1

### Small Amplitude Oscillatory Shear Flow and Steady Shear Flow:

$$G'(\omega) = \sum_i \frac{G_{oi}\lambda_i 2\omega^2}{(1+\lambda_i 2\omega^2)} \quad (11) \quad G''(\omega) = \sum_i \frac{G_{oi}\lambda_i \omega}{(1+\lambda_i 2\omega^2)} \quad (12)$$

$$\eta(\dot{\gamma}) = f \sum_i \frac{G_{oi}\lambda_i}{(1+n_1\dot{\gamma}\lambda_i)^2} + (1-f) \sum_i \frac{G_{oi}\lambda_i}{(1+n_2\dot{\gamma}\lambda_i)^2} \quad (13)$$

### Start-up Flow and Cessation of Steady Shear Flow:

$$\eta^+(t, \dot{\gamma}) = f \sum_i \frac{G_{oi}\lambda_i}{(1+n_1\dot{\gamma}\lambda_i)^2} \left[ 1 - \exp(-t_{1,i})(1 - n_1\dot{\gamma}\lambda_i t_{1,i}) \right] + (1-f) \sum_i \frac{G_{oi}\lambda_i}{(1+n_2\dot{\gamma}\lambda_i)^2} \left[ 1 - \exp(-t_{2,i})(1 - n_2\dot{\gamma}\lambda_i t_{2,i}) \right] \quad (14) \text{ where}$$

$$t_{1,i} = \frac{1 + n_1 \dot{\gamma} \lambda_i}{\lambda_i} t \quad \& \quad t_{2,i} = \frac{1 + n_2 \dot{\gamma} \lambda_i}{\lambda_i} t \quad \text{and} \quad \eta^+(t, \dot{\gamma}) = \frac{\tau_{12}^+(t, \dot{\gamma})}{\dot{\gamma}}$$

$$\eta^-(t, \dot{\gamma}) = \sum_i \left[ (f G_{oi} \lambda_i) / (1 + n_1 \dot{\gamma} \lambda_i)^2 + (1 - f) G_{oi} \lambda_i / (1 + n_2 \dot{\gamma} \lambda_i)^2 \right] \exp(-t / \lambda_i) = \frac{\tau_{12}^-(t, \dot{\gamma})}{\dot{\gamma}} \quad (15)$$

**TABLE 2**

Relaxation Time  $\lambda_i$  and Strength  $G_{oi}$  at T=90\_C

$\lambda_i, s$	$G_{oi}, Pa$
1000	1.00E-04
100	2.00E-02
10	7.42E-01
1	1.82E+02
0.1	1.82E+03
0.01	2.38E+04

**TABLE 3**

Parameters in Double Exponential-Type Damping Function

<b>f</b>	0.0870
<b>n1</b>	1E-05
<b>n2</b>	0.1627

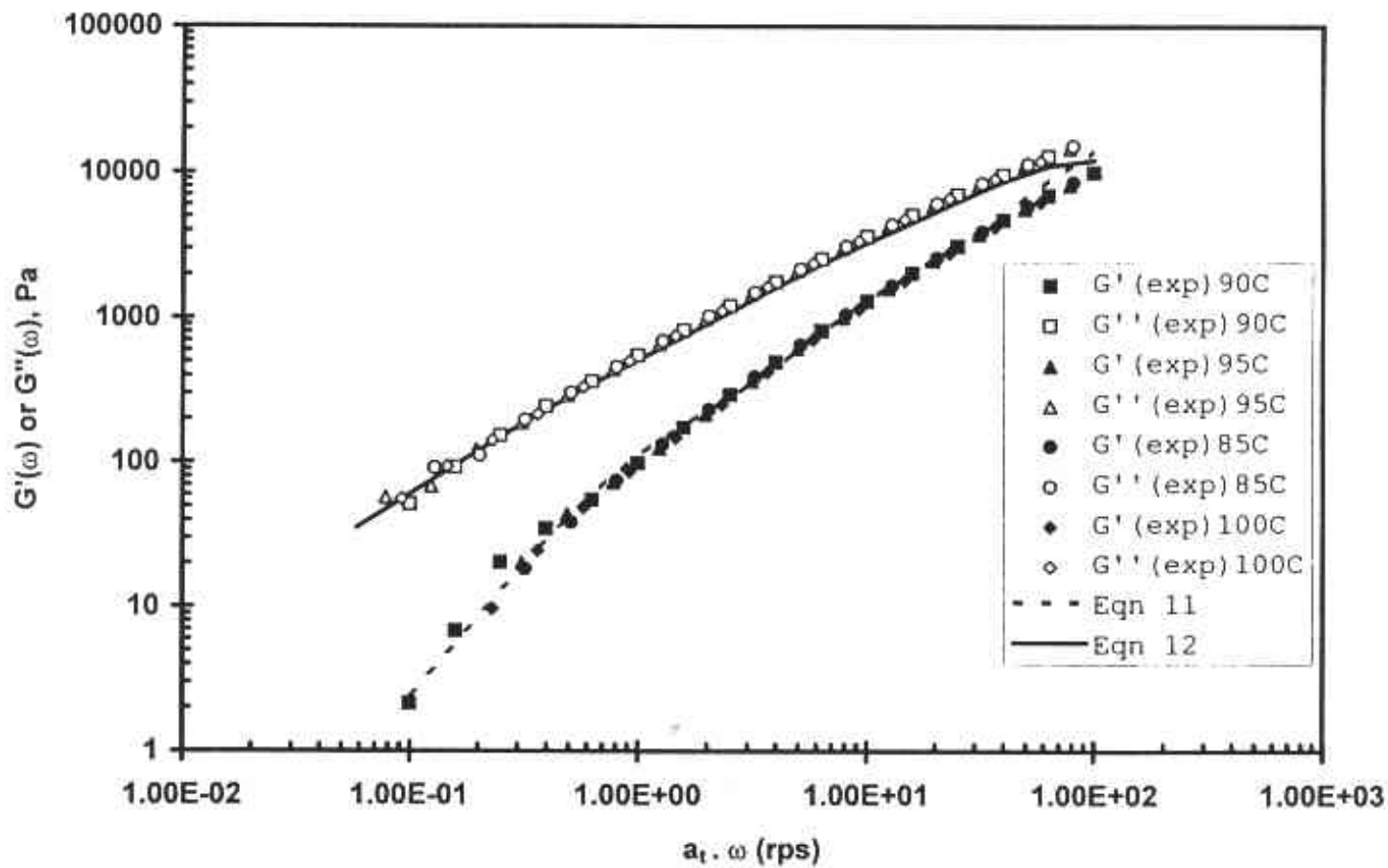


Fig. 1. Storage and loss moduli of 25% BAMO-AMMO

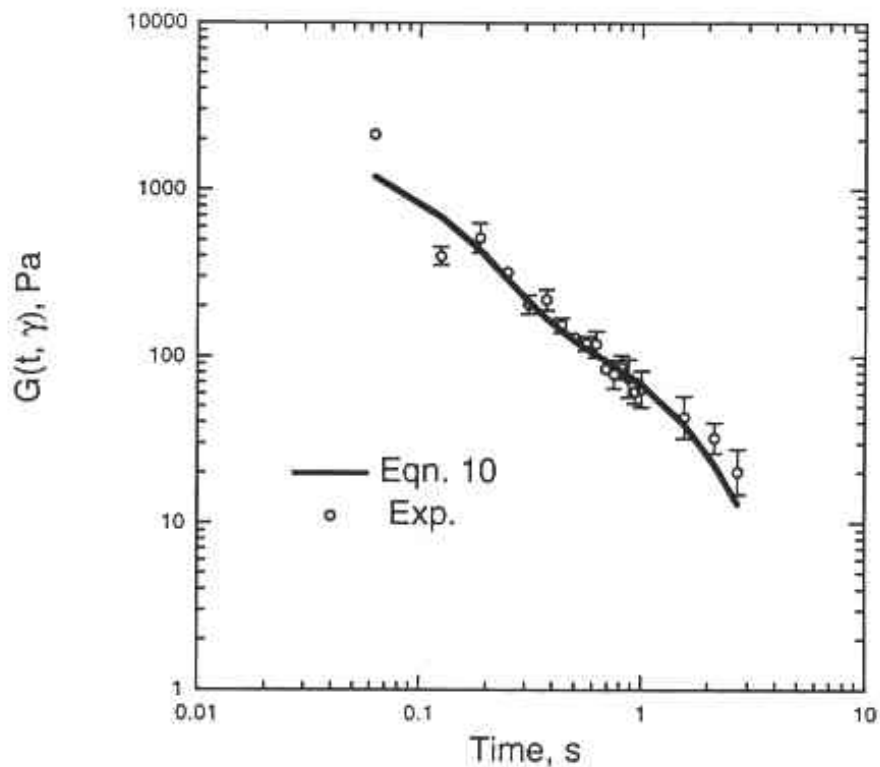


Fig. 2. Typical confidence intervals of the relaxation moduli in the linear viscoelastic range

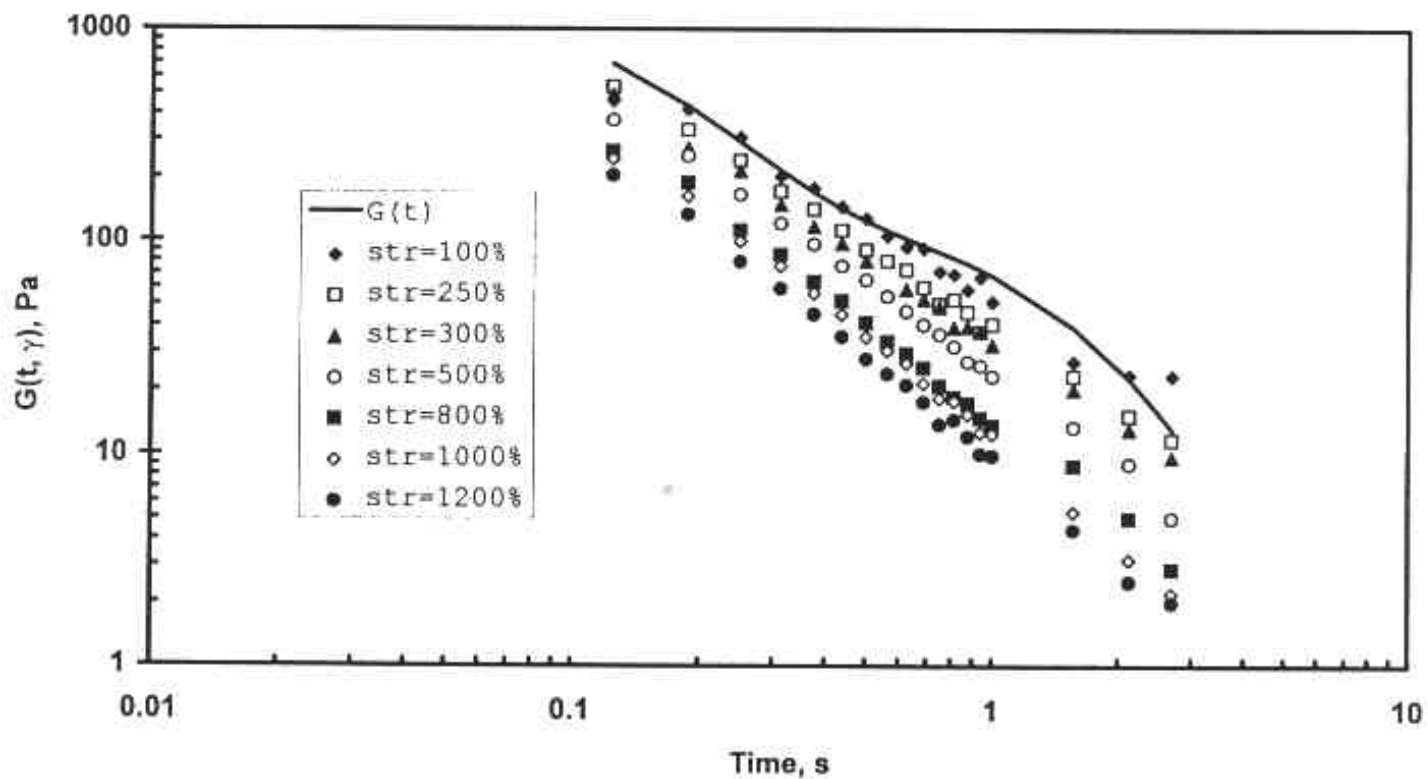


Fig. 3. Shear relaxation modulus of 25% BAMO-AMMO

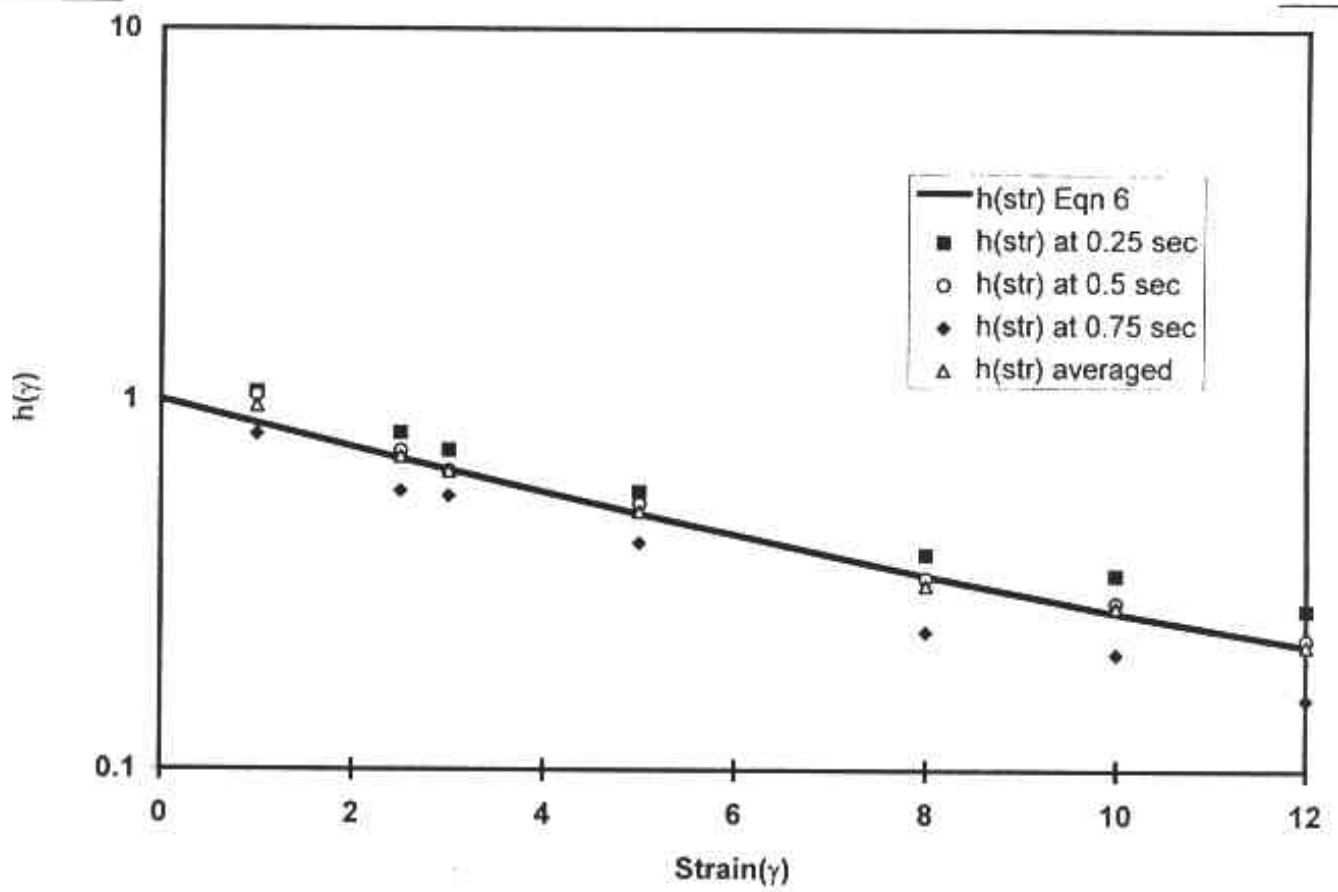


Fig. 4. Strain dependence of the damping function

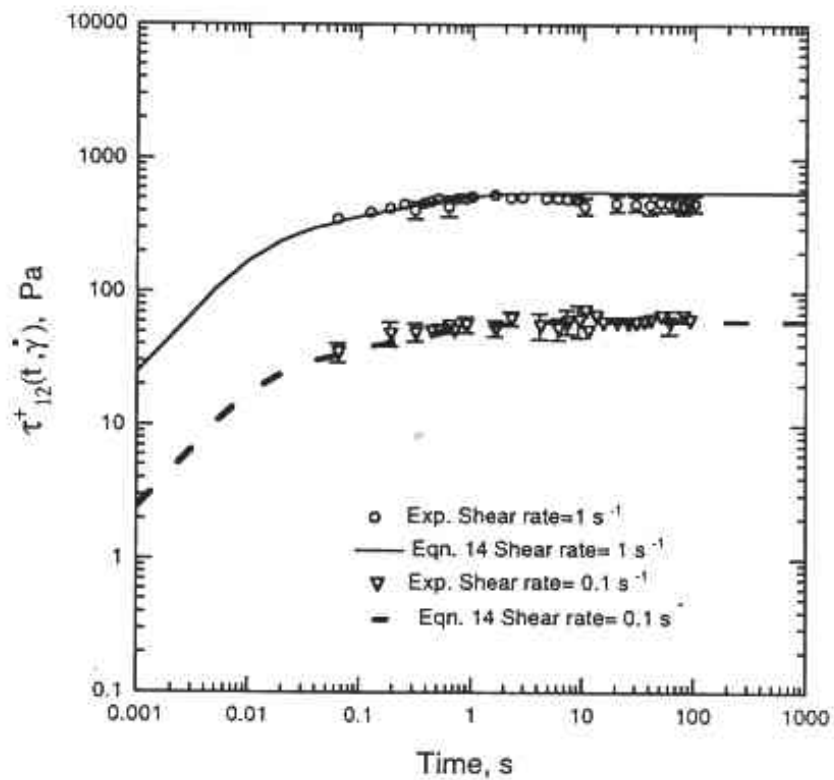


Fig. 5. Shear stress growth

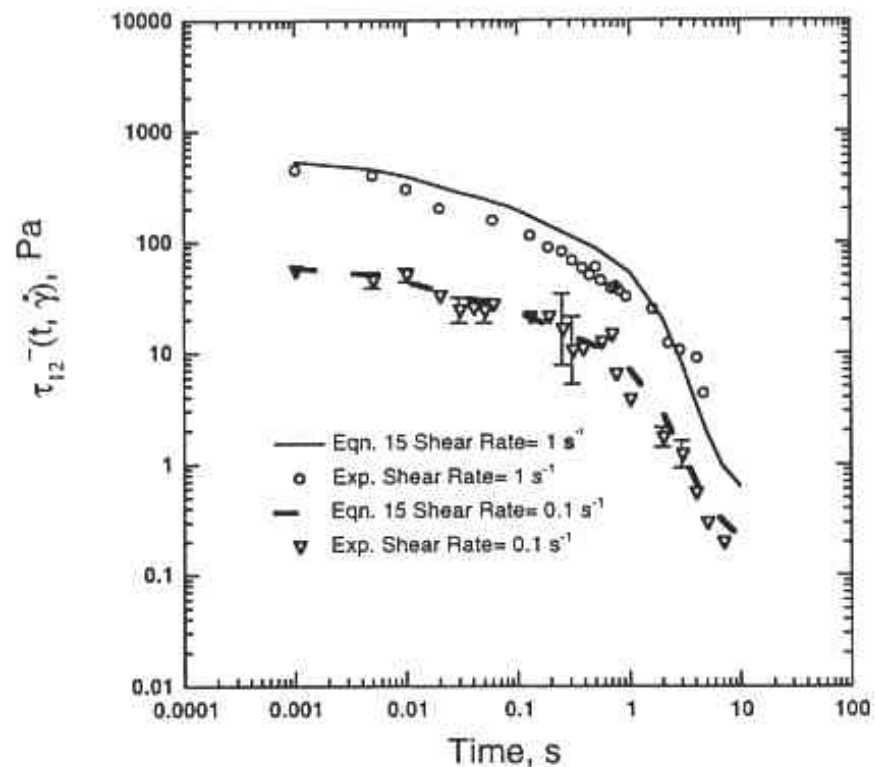


Fig. 6. Shear stress relaxation upon the cessation of steady shear

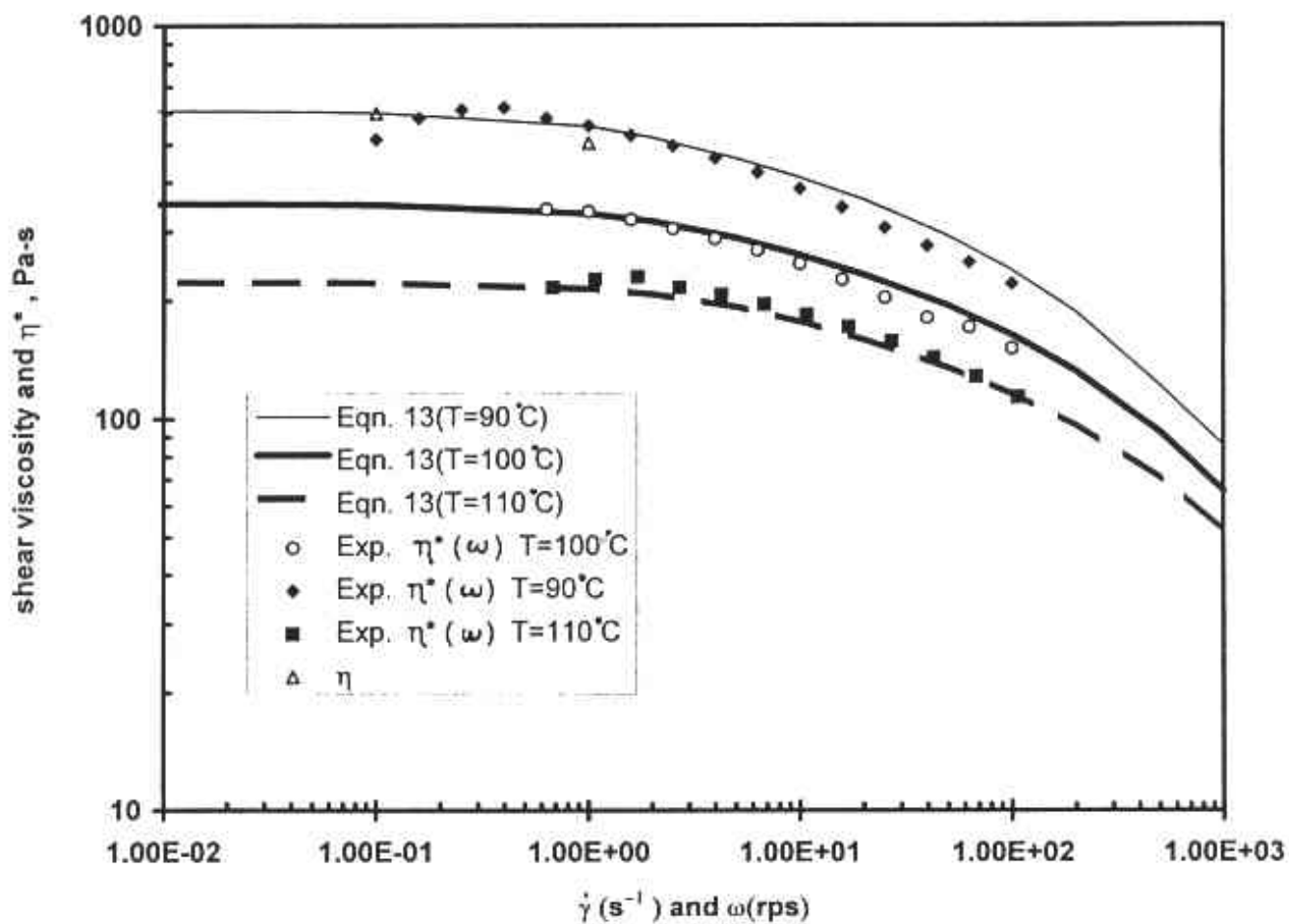


Fig. 7. Shear viscosity and magnitude of complex viscosity